



Use of phosphogypsum - tar based material in the manufacture of building products

S. Chouaya^{1,3}, M. A. Abbassi², R. Ben Younes³, S. Abderafi⁴

¹Tunisian Chemical Group (GCT), M'dhilla, Gafsa, Tunisia.

²UR: Materials Research Unit, Energy and Renewable Energy (MEER),
Faculty of Sciences of Gafsa, B.P.19, Zarroug, Gafsa, 2112, Tunisia.

³UR: Physics, Informatics and Mathematics Research Unit (PIM),
Faculty of Sciences of Gafsa, B.P.19, Zarroug, Gafsa, 2112, Tunisia.

⁴Mohammadia Engineering School, Mohammed V University in Rabat,
Ibn Sina, B.P. 765, Agdal, Rabat, 10090, Morocco.

Received 12 Oct 2019,
Revised 20 Nov 2019,
Accepted 21 Nov 2019

Keywords

- ✓ Phosphogypsum,
- ✓ Tar,
- ✓ Tire pyrolysis,
- ✓ Compressive strength

chouayasana15@gmail.com

Phone: +216 21 284 509;

abbassima@gmail.com

Phone: +216 95 577 005

Abstract

With the growing awareness of environmental issues, much research is currently devoted to the development of new solutions. The present work aimed to study the potential use of phosphogypsum (PG) which is a byproduct of the phosphoric acid production units. PG was characterized using chemical analysis, scanning electron microscopy, X-ray diffraction, infrared spectrum and thermogravimetric analysis. It was found that washing with water and heat treatment minimizes soluble and volatile impurities. Subsequently, a PG-tar-based binding material was prepared by mixing 40% PG, 50% tar and 10% caustic soda. A series of mechanical tests were conducted to determine the compressive strength of the prepared specimens. Results show that the compressive strengths of pastes prepared with treated PG are slightly higher than those prepared with raw PG. Based on the test results, it can be concluded that the obtained binder material can be used for the production of interior wall materials such as bricks and blocks.

1. Introduction

Solid waste constitutes a significant portion of hazardous materials [1-3]. It is a major environmental issue in many countries worldwide. Phosphogypsum (PG), which is an acidic by-product of the phosphate fertilizer industry, is one of the notorious wastes. About 5 tons of PG are produced per ton of phosphoric acid [3-5]. The annual PG production in Tunisia is currently estimated at 10 million tons for the five phosphoric acid production plants belonging to the Tunisian Chemical Group (TCG). The stockpiles of PG pose various environmental and storage problems. They contain impurities of free phosphoric acid, fluorides, phosphates and organic matter that adhere to the surface of gypsum crystals and also integrate in the crystal lattice of gypsum [3-6]. Disposing of this waste without any prior treatment into the environment as piles exposed to weathering processes may lead to chemical and radioactive contamination. In order to make PG harmless and suitable for later applications, researchers have proposed several methods, such as washing and heat treatment [3,7-12]. Taher et al. [8] focused their work on the heat treatment of Egyptian PG to make it suitable for the manufacture of Portland cement. The heat-treated PG was found to contain fewer phosphorus pentoxide (P_2O_5) impurities, less fluoride and organic matter than the raw PG. The scanning electron microscopy (SEM) micrographs given by Tayibi et al.[3] reveal a homogeneous and prismatic stacking distribution. The Infrared (IR) spectra of PG sample highlight that there are many vibrational absorption bands, characterized mainly by inorganic sulfur compounds [13,14]. Furthermore,

X-ray diffraction (XRD) analysis show three strong peaks at diffraction angles of 14.7 ($d=6.02\text{\AA}$), 25.7 ($d=3.5\text{\AA}$) and 29.8 ($d=3\text{\AA}$). These are attributed to gypsum ($\text{CaSO}_4 \cdot 2\text{H}_2\text{O}$) with small amounts of silica and metallic impurities, such as Na, Al, Fe, and Sr. This is consistent with the spectroscopic characterization reported by El-Didamony et al. [4]. The thermogravimetric analysis (TGA) and differential thermogravimetric (DTG) studies confirm that temperature and kinetic dehydration of hydrated calcium sulfate could be influenced by several parameters such as sample origin, chemical composition and crystalline structure [15-18]. In the literature, different PG recovery processes have been proposed. For example, Huang et al. [13] prepared a binder based on 45% PG, 48% slag and 7% cement clinker with a chemical activator of 1% which has a compressive strength comparable to that of silicate cement [13]. Another study by Yang et al. [11] proposes the use of raw PG in the preparation of self-leveling mortar. Ajam et al. [18] investigated the incorporation into different mass percentages of PG with sand and cement in the manufacture of raw bricks by obtaining that with 30% PG the bricks successfully met the standard requirements. These ways of valorization constitute new perspectives which can be an effective solution to environmental problems caused by the huge amounts of PG.

This present study aimed to prepare a binding material using two wastes: phosphogypsum and tar obtained from pyrolysis of used tires described in a previous study by Chouaya et al. [19].

We performed various tests in the laboratory, to propose an optimal composition of the mixture of PG, tar and caustic soda (NaOH). By following different analyses, it was proven that PG treated material can be upgraded to a high added value product.

2. Material and Methods

2.1. Samples

The basic ingredients of this research were Gafsa-M'dhillia PG, tire pyrolysis tar (TPT)[19] as well as natural and commercial gypsums that were used as a reference.

The samples of PG were obtained after the transformation of phosphate deposits in Gafsa basin, in the south-west of Tunisia. **Figure.1.a** shows stockpiles of PG in the region of Gafsa-M'dhillia and **Figure.1.b** illustrates soil contamination around these stockpiles.



Figure.1.a: Stockpiles of PG in the region of Gafsa-M'dhillia



Figure. 1.b: Soil contamination around the stockpiles of PG in the region of Gafsa-M'dhillia

The raw PG was treated to remove additional water and impurities by washing, filtration, grinding, and oven drying. It was washed by water, ground and thermally treated at 140–150°C for 30 min and at 130–150°C for 60 min. Then, the treated PG was desiccated in a closed vessel at room temperature to avoid any contamination. This method was used because it is the most suitable and the cheapest. Tire pyrolysis tar (TPT) is a collected liquid in pyrolysis of scrap tires in a mini-pyrolyzer designed in our laboratory [19].

2.2. Characterization methods:

PG samples were observed and characterized using a JEOL IT 100 scanning electron microscope (SEM). This technique makes it possible to visualize a sample and determine its size, crystalline form and the appearance of the crystals.

The ultimate analysis, determined using an Elemental Analyzer Flash 2000, indicated the amount of carbon, hydrogen, nitrogen, sulfur and oxygen of the different samples.

For electrical conductivity measurement, PG was washed using 15g of PG powder mixed with 30 ml of water in a beaker at $T = 25^{\circ}\text{C}$ in a magnetic stirrer. After 40 min, the solution was filtered and the pH and the filtrate conductivity were measured. The same process was repeated several times. To measure the electrical conductivity of the samples we used a conductivity meter WTW LF 530 model characterized by a very wide measuring range between 0 and 1999 mScm^{-1} , conductivity accuracy ± 0.005 and conductometric cells type TACUSSEL constants 0.1; 1 to 10 cm^{-1} . The evolution of the pH during the washing of PG was monitored using a 780 pH Meter from Metrohm with pH accuracy equal to ± 0.003 .

The functional group composition analysis of commercial gypsum, raw and treated PG was carried out using Fourier Transform Infrared spectroscopy (FT-IR) analyzer (SHIMADZU FT-IR-8400S) within $400\text{--}4000\text{ cm}^{-1}$ with 4 cm^{-1} resolution. The X-ray diffraction analysis was conducted to determine the mineralogical composition of M'dhilla PG. The powder diffraction pattern of the sample was obtained with $\text{Cu K}\alpha$ radiation and Ni filter. The scanning speed was $2\Theta = 1\text{ deg./min}$, at constant voltage 40 kV and 30 mA using PW 1390 X-ray diffractometer. The identification of the minerals was carried out using the data given in the ASTM cards by measuring the d -values of the different atomic planes and their relative intensities.

The thermal analyzer (SETSYS EVOLUTION TGA-DTA/DSC) was used to obtain thermogravimetric analysis (TGA) and differential thermogravimetric (DTG) data of the prepared samples of M'dhilla PG and commercial gypsum which were heated over the temperature range of $25\text{--}800^{\circ}\text{C}$ at constant heating rates of 10°C/min in a high purity N_2 atmosphere with a flow rate of 20 ml/min .

2.3 Mixing and preparation of compression specimens:

For specimen preparation, we performed compression tests on raw and treated PG samples as well as mix proportions of PG-tar of tire pyrolysis based material. These compression specimens were cast in parallelepiped molds of (40.0mm, 40.0mm and 160.0mm). After being removed from the molds, they were kept under atmospheric pressure and average room temperature. A large number of specimens were made with different proportions of PG, caustic soda and TPT. Raw and treated PG were used in preparing the mix proportions of the compression specimens.

Different compositions of the PG-TPT-based material mixture can be used, (Table 1). The percentages are expressed by weight in dry material mixtures. After several mixing tests of M1 to M6, we chose the mixture (M5) which is composed of 40% PG, 50% tar and 10% caustic soda. Indeed, we have targeted at least a pH of 7 and the M5 mixture was chosen, to avoid the risk of contamination of the subsoil by the different impurities.

Table1: Mix proportions of the PG-TPT-based material (%)

Mixture materials (%)	PG	TPT	NaOH
M1	0	90	10
M2	10	80	10
M3	20	70	10
M4	30	60	10
M5	40	50	10
M6	50	40	10

The compressive strength tests of the studied PG-tar of tire pyrolysis based material were performed at 28 days in conformance with TS EN 196. Its measurements were carried out using PROETI.S.A, hydraulic unit C0123 automatic servo-controlled press with a capacity of 300 kN.

3. Results and discussion

3.1 Scanning electron microscopy

PG samples are studied at by Scanning electron microscopy (SEM). The results of the SEM observation of the raw PG samples are shown in **Figure 2**. The micrographs reveal a homogeneous and prismatic stacking

distribution. They have a well-defined crystalline structure with a majority of rhombic and orthorhombic crystals. The predominant phase in this group is gypsum crystals in the form of platelets distributed in the matrix of calcium sulfate.

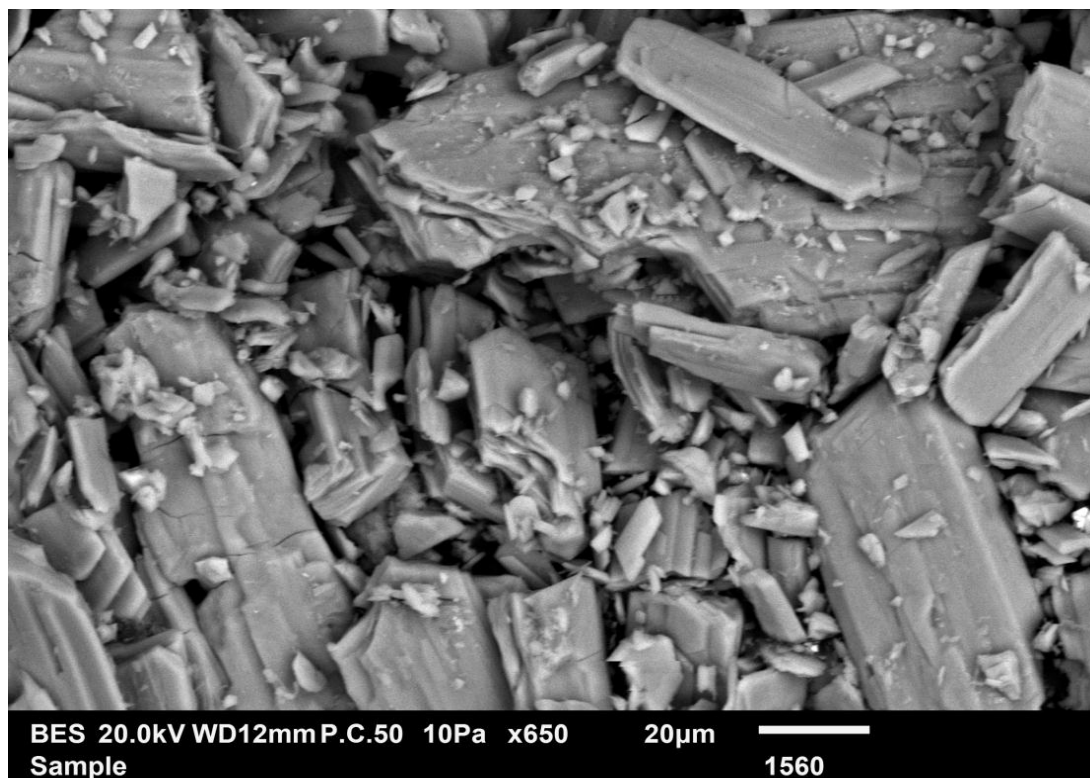


Figure 2: SEM image of PG sample studied at (x400, 20µm)

3.2. Chemical composition

The chemical composition of the raw PG, treated PG and natural gypsum samples are summarized in **Table 2**. The ultimate analysis indicated a high amount of oxygen in PG. This can be explained by the presence of highly oxygenated compounds as well as sulfur compounds from the microorganisms present in the sedimentation. The atomic ratio (H/C) of TPT was around 1.4. This value indicates that it is a mixture of aliphatic and aromatic compounds derived from polymeric materials [19]. As expected, the main contents of PG are Ca and S (expressed as CaO and SO₃, respectively), which together make more than 80 wt.%. The rate of P₂O₅ is relatively high. This can be related to the poor filtration of the gypsum cake after the reaction attack of phosphate rock by sulfuric acid. There are other impurities such as iron oxides, magnesium, aluminum, sulfide, organic matter and trace metals [5]. According to the results of the chemical composition of the treated PG and the natural gypsum; they had similar chemical compositions with minor differences in some values.

Table 2: Chemical composition of PG, treated PG, natural gypsum and TPT

	Elemental Analysis (wt.%)					CaO (%)	P ₂ O ₅ (%)	Mg (%)	SiO ₂ (%)	SO ₃ (%)	MgO (%)	Cd ppm	Corg (%)
	C	H	N	S	O								
PG	0.371	1.655	-	9.275	88.7	36.62	7.38	1.62	1.83	44	0.66	11.90	0.22
Treated PG	0.339	0.635	-	9.889	89.137	38.36	1.82	0.07	0.70	42	0.08	2.32	0.25
Natural gypsum	0.143	0.053	-	17.353	82.451	37.82	-	-	1.90	42	-	-	-
TPT[19]	86.20	10.70	0.50	1.20	1.40	-	-	-	-	-	-	-	-

3.3 Electrical conductivity measurement

The evolution of the electric conductivity and pH during the washing of PG, taking into account measurement errors during experimental tests, is illustrated in **Figure 3**. The dissolution leads to an increase in the pH value from 2.2 to 6. Whereas it is noted that there is a rapid decrease in the conductivity along with the washing number until reaching a constant value equal to 2.1. These two values (pH=6 and conductivity=2.1 mS/cm) are comparable to those of the solution ($\text{CaSO}_4 \cdot \text{H}_2\text{O}$) of pure natural gypsum taken as a reference.

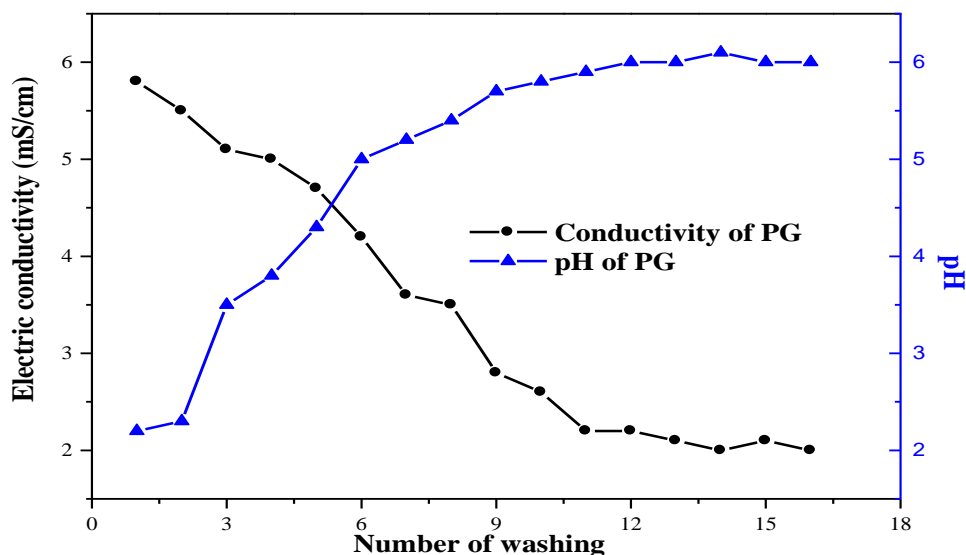


Figure 3: Evolution of the electric conductivity and pH during the washing of PG

3.4 Spectroscopic characterization of PG

The IR spectra of different samples of commercial gypsum, raw and treated PG have been measured as potassium bromide (KBr) disc. The spectra of PG show that there are many vibrational absorption bands (**Figure 4**). In this respect, the strong absorption band at $\sim 1125 \text{ cm}^{-1}$ is attributed to stretching vibrations of SO related to the sulfate group as calcium sulfate in PG waste sample. Also, there are strong absorption bands at $\sim 3562 \text{ cm}^{-1}$ and 1620 cm^{-1} which are related to the OH group of moisture content in PG.

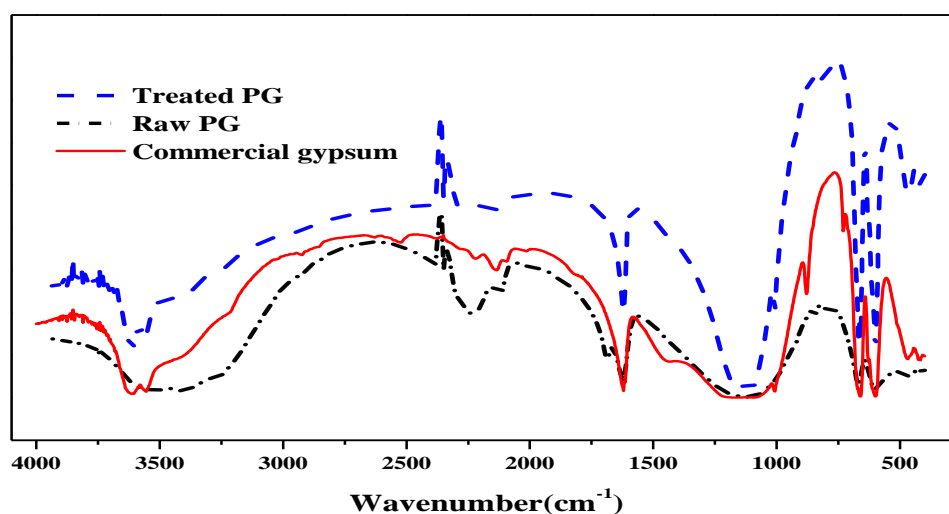


Figure 4: IR Spectroscopy of commercial gypsum, raw and treated PG

The absorption bands at 2225 cm^{-1} and 2140 cm^{-1} are attributed to POH stretching of the phosphoric acid residue in PG wastes. The vibrations at 662 cm^{-1} , 600 cm^{-1} and 466 cm^{-1} are due to M–O band which is related to the presence of metal-oxides content in PG [4, 14]. However, from the spectra shown in **Figure 4**, we can deduce that the treated PG has no P_2O_5 in the crystal lattice, whereas the other PG sample has P_2O_5 in a co-crystalline form that is shown as weak absorptions at about 840 cm^{-1} .

The X–ray diffraction pattern of M’dhilla PG sample is presented in **Figure 5**. The spectrum shows the three main strong peaks at diffraction angles of 12° ($d = 7.499\text{ \AA}$), 21° ($d = 4.276\text{ \AA}$) and 29.4° ($d = 3.064\text{ \AA}$), which are assigned to bassanite ($\text{CaSO}_4 \cdot 0.5(\text{H}_2\text{O})$), which is the predominant phase in these compositions, an anhydrite (CaSO_4) which is characterized by a peak observed at 23.5° ($d = 3.799\text{ \AA}$) and quartz at 26.5° ($d = 3.338\text{ \AA}$). The other weak peaks are attributed to the presence of minor phases, namely silicate, phosphate and metallic impurities, such as Na, Al, Fe, and Sr. These results are in line with those of Didamony et al.[4].

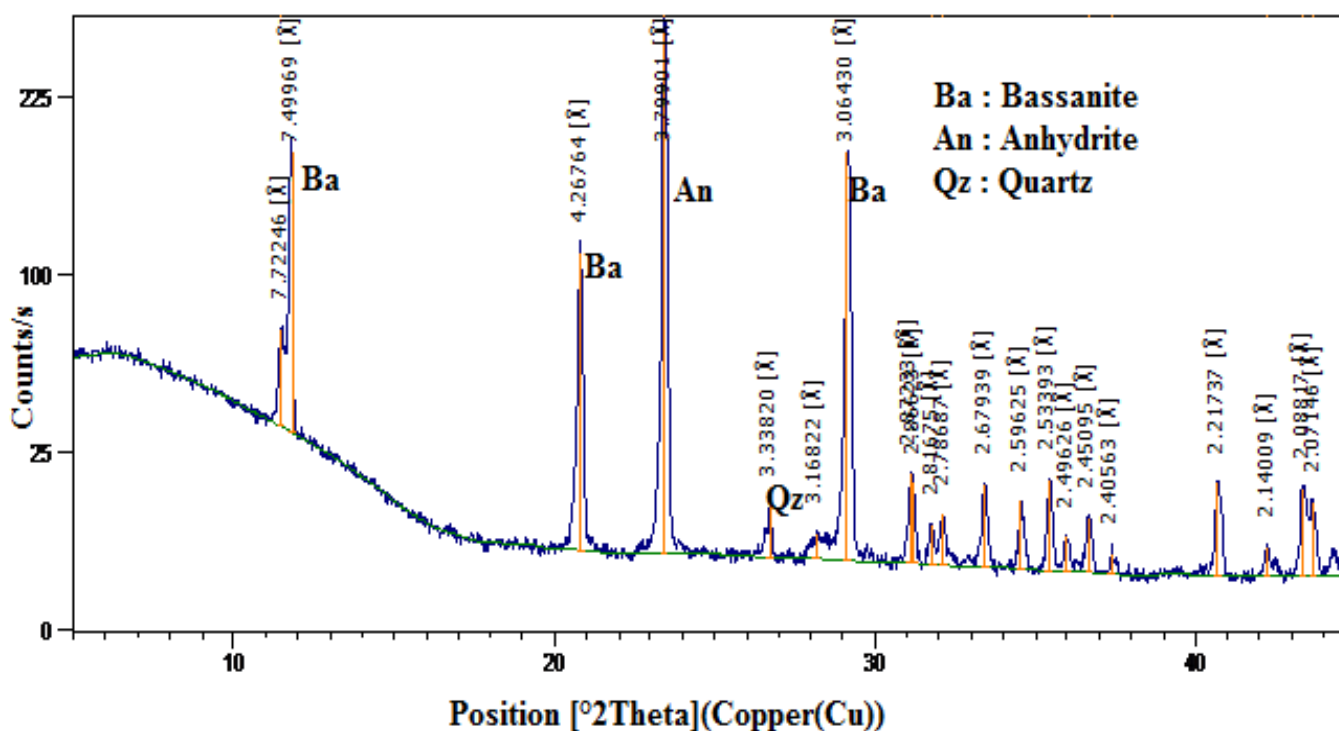


Figure 5: Spectrum of the X-ray diffraction of M’dhilla PG

3.5 Thermogravimetric analysis of M’Dhilla PG

The thermogravimetric analysis of M’dhilla PG at $10^\circ\text{C}/\text{min}$ is represented in **Figure 6**. The obtained TG curve shows two different mass loss stages. The first mass loss, which is between 138°C and 172°C , represents 4.6% of the initial mass (26.42mg) and is due to the elimination of the hydration water. The second one starts at 172°C and ends at 232°C . It corresponds to the formation of the anhydrite III, which is observed on the TG curve by a change in the slope and on the derived curve by an accentuated peak. Thus, we notice a total loss of 8.6% of the initial mass at 600°C . The derived curve shows two consecutive endothermic peaks between 166°C and 182°C for the raw PG sample. These peaks are related to the modifications of the crystalline structure. The first endothermic peak corresponds to the gypsum dehydration reaction and the formation of the hemihydrate according to Eq.1 (**Table 3**). The second peak observed is attributed to the transformation of hemihydrate into anhydrite III, according to the reaction in Eq.2 (**Table 3**). The third peak occurs at 432°C and corresponds to a slightly exothermic reaction in Eq.3 (**Table 3**). It is the result of the crystallographic transformation of soluble anhydrite III into insoluble anhydrite II. At this temperature, we notice no mass loss on the TG curve. **Table 3** reports the results for each peak and the thermal transformation of raw PG.

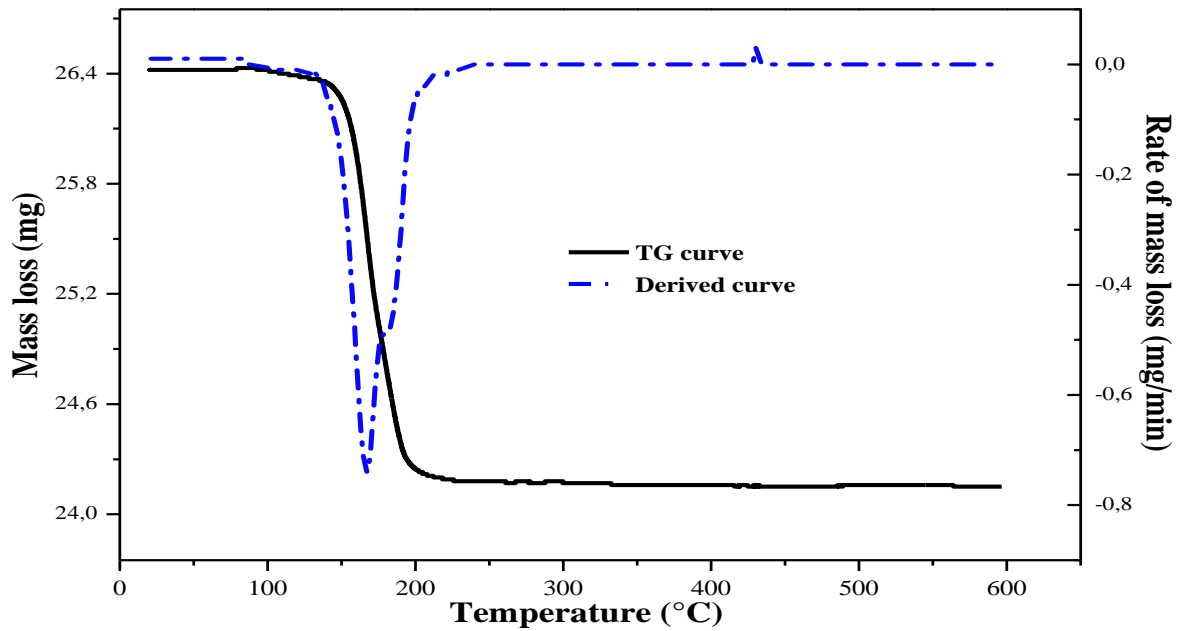


Figure 6: TG and derived curves of M'dhilla PG at 10°C/min

Table 3: Thermal transformation of raw PG

Peak	Tp (°C)	Reaction	Nature
1 st	166	$\text{CaSO}_4 \cdot 2\text{H}_2\text{O} \rightarrow \text{CaSO}_4 \cdot \frac{1}{2}\text{H}_2\text{O} + \frac{3}{2}\text{H}_2\text{O}$ Eq.1	Endothermic
2 nd	182	$\text{CaSO}_4 \cdot \frac{1}{2}\text{H}_2\text{O} \rightarrow \text{CaSO}_4\text{III} + \frac{1}{2}\text{H}_2\text{O}$ Eq.2	Endothermic
3 rd	432	$\text{CaSO}_4\text{III} \rightarrow \text{CaSO}_4\text{II}$ Eq.3	Exothermic

Tp : maximum temperature peak

These results are consistent with those of previous studies that show the presence of two endothermic peaks. However, the corresponding temperatures have been quite varied. Lopez et al.[15] have obtained a double peak at 156°C and 191°C for Tunisian PG and 144°C and 175°C for Spanish PG, respectively. While in Sebbahi et al. [16], the two endothermic peaks appear respectively at 66 and 133°C with another endothermic peak at 1184°C which was not identified in the present study. **Figure 7** shows the profile of the dehydration of commercial gypsum at 10°C/min. It shows a single endothermic peak at a maximum temperature of 150°C which extends from 90°C to 170°C. This finding is in line that found by Cuadri et al. [17], who obtained a peak which extends from 90 to 170°C with a maximum temperature of 130°C. The thermal behavior curves show a difference in the dehydration temperature that might be explained by the effect of nature and the surrounding area as well as the difference in the origins and chemical composition of the samples.

3.6 Compression tests on raw and treated M'Dhilla PG

The compression was performed on raw and treated PG specimens. The test pieces were crushed for three months with a time interval of 10 days. **Figure 8** shows the evolution of resistance with age, with each point representing the average of three trials. As can be seen from this figure, most of the resistance develops during the first ten days of the life of the specimens, but continues overtime. The lowest values of compressive strength are observed on all samples containing raw PG. However, treated PG increased the mechanical properties of the specimens. In

order to improve the resistance, we propose to use tar of tire pyrolysis. **Figure 9.a** shows a view of test specimens that were made of tire pyrolysis tar and PG (raw and treated).

The comparison of the compressive strength of specimens with raw and treated PG-TPT-based material is shown in **figure 9.b**. The compressive strength of pastes M5-Raw PG and M5-Treated PG is almost the same after 3 days. Only the compressive strengths of pastes with Raw PG are slightly lower than those with Treated PG at 7 and 28 days.

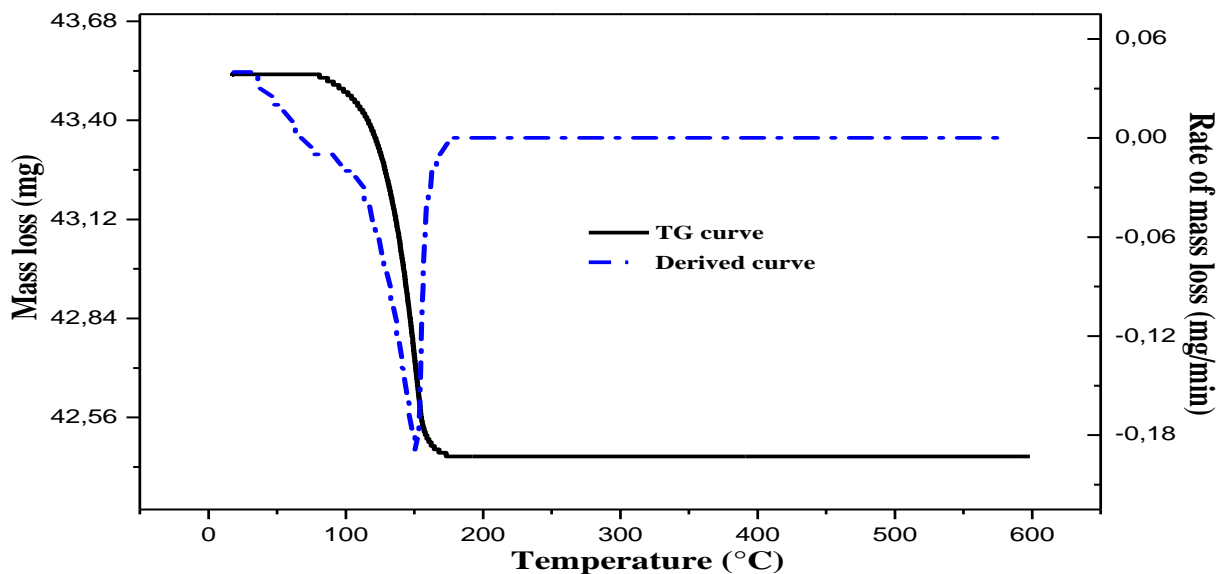


Figure 7: TG and derived curves of commercial gypsum at 10°C/min

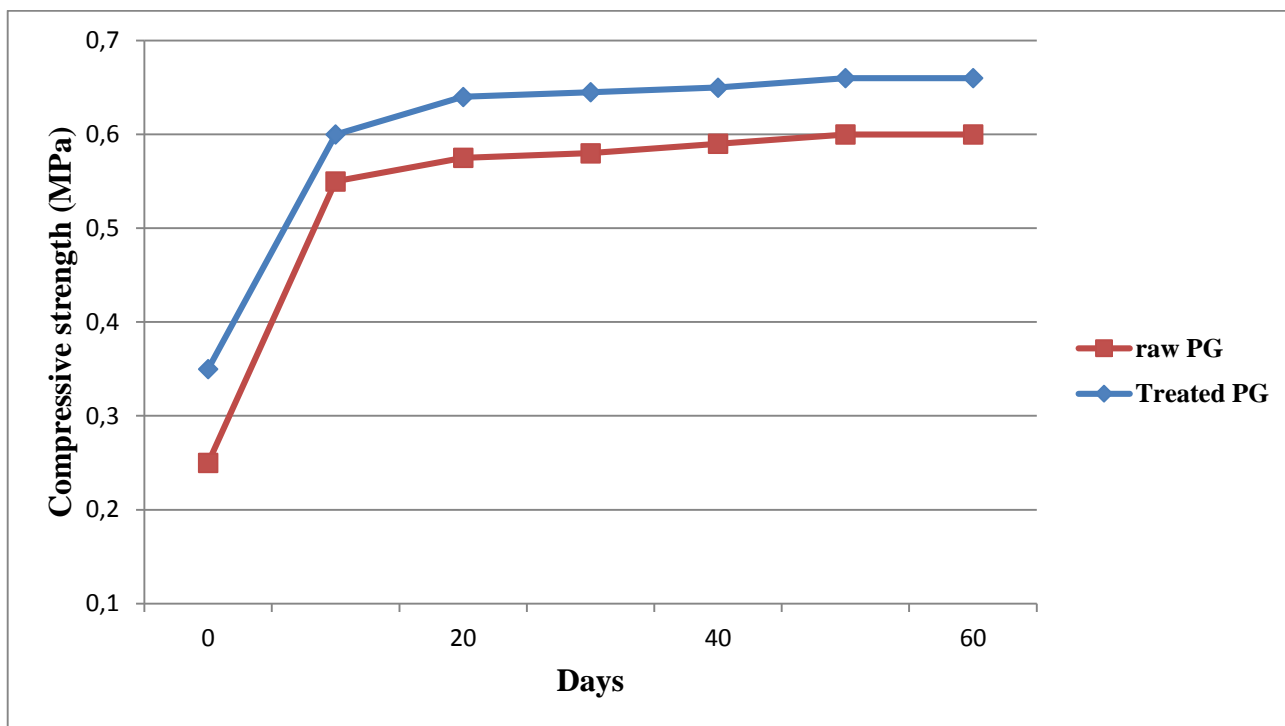


Figure 8: Compressive strength of raw and treated PG samples



Figure 9.a: A view of specimens with raw and treated PG-TPT- based material

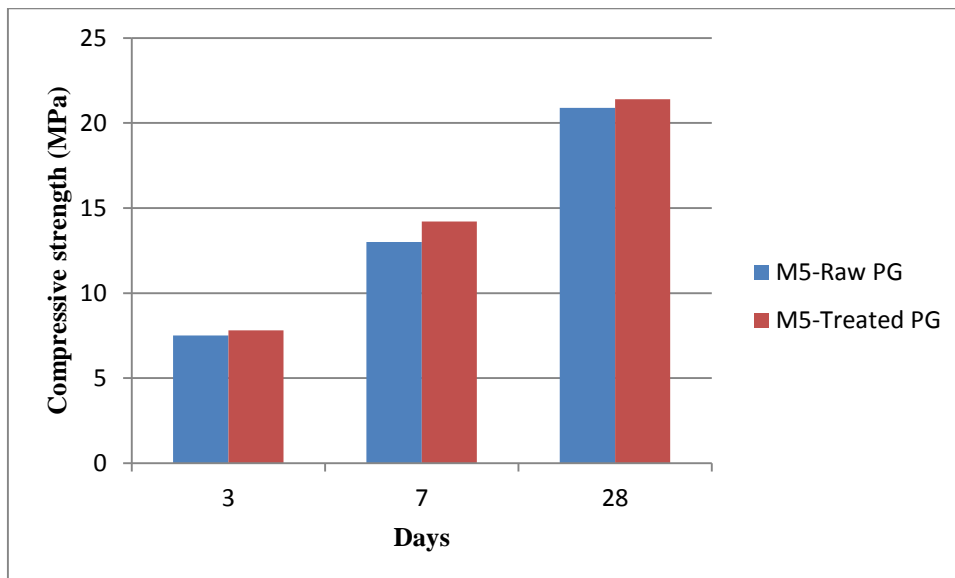


Figure 9.b: Compressive strength of mix proportions M5 with raw and treated PG

Conclusion

The present paper highlights the results of the characterization and valorization of raw and treated PG. Based on the experimental results of this investigation several conclusions can be drawn:

- Solid PG waste samples produced in a plant for fertilizer and phosphoric acid production were characterized using spectroscopic measurements. It can be concluded from the chemical composition, XRD and IR measurements that the main phase composition of the studied PG is dehydrated calcium sulfate ($\text{CaSO}_4 \cdot 2\text{H}_2\text{O}$).
- All the water-soluble impurities can be removed by washing with water. Furthermore, all the impurities in the crystal lattice can be removed by thermal treatment. The heat-treated PG contains fewer P_2O_5 impurities, fluoride and organic matter than the raw PG. Hence, the treatment with water permits to remove soluble impurities and the thermal treatment leads to optimize the removal of volatile impurities.
- Heat treatment and washing by water of phosphogypsum have resulted in the highest improvement in the compressive strength of the specimens.
- The phosphogypsum-tar-based binding material was prepared by mixing 40% phosphogypsum, 50% tar and 10% caustic soda. The results of the compressive strength show that the obtained composite materials have good performances. It is an appropriate alternative composite material and that can be used widely in infrastructure building.

Acknowledgement-We would like to thank the scientific and technical council of Tunisian Chemical Group (GCT), the National Engineering School of Gabes, Physics, Informatics and Mathematics Research Unit (UPIM) in Gafsa and Research Center of Metlaoui for their technical assistance.

References

1. R. El Zrelli, L. Rabaoui, N. Daghbouj, H. Abda, S. Castet, S., Josse, P. Courjault-Radé, Characterization of phosphate rock and phosphogypsum from Gabes phosphate fertilizer factories (SE Tunisia): high mining potential and implications for environmental protection. *Environmental Science and Pollution Research*, 25(15) (2018) 14690-14702.
2. H. Bensalah, Bekheet, M. F., Younssi, S. A., Ouammou, M., & Gurlo, A. Hydrothermal synthesis of nanocrystalline hydroxyapatite from phosphogypsum waste. *Journal of environmental chemical engineering*, 6(1) (2018) 1347-1352.
3. H. Tayibi, M. Choura, M., López, F. A., Alguacil, F. J., & López-Delgado, A. Environmental impact and management of phosphogypsum. *Journal of environmental management*, 90(8) (2009) 2377-2386.
4. H. El-Didamony, H. S. Gado, N. S. Awwad, M. M. Fawzy, M. F. Attallah, Treatment of phosphogypsum waste produced from phosphate ore processing. *Journal of Hazardous Materials*, 244 (2013) 596-602.
5. Guo, Tingzong, Ronald F. Malone, and Kelly A. Rusch. Stabilized phosphogypsum: class C fly ash: Portland type II cement composites for potential marine application. *Environmental Science & Technology*, 35(19) (2001) 3967-3973.
6. N. Mechi, Khiari, R., Ammar, M., Elaloui, E., & Belgacem, M. N. Preparation and application of Tunisian phosphogypsum as fillers in papermaking made from *Prunus amygdalus* and *Tamarisk* sp. *Powder Technology*, 312 (2017) 287-293.
7. Nehdi, Moncef, and Ashfaq Khan. Cementitious composites containing recycled tire rubber: an overview of engineering properties and potential applications. *Cement, concrete and aggregates*, 23(1) (2001) 3-10.
8. M. A. Taher, Influence of thermally treated phosphogypsum on the properties of Portland slag cement. *Resources, Conservation and Recycling*, 52(1) (2007) 28-38.
9. N. Mechi, Ammar, M., Loungou, M., & Elaloui, E. (2016). Thermal study of Tunisian phosphogypsum for use in reinforced plaster. *British Journal of Applied Science & Technology*, 16(3) (2016) 1-10.
10. S. Hassen, Anna, Z., Belgacem, M. N., & E. Mauret, Study of the valorization of phosphogypsum in the region of Gafsa as filler in paper. In *IOP Conference Series: Materials Science and Engineering*, 28. 1 (2012).
11. L. Yang, Zhang, Yunsheng, Yan, Yun. Utilization of original phosphogypsum as raw material for the preparation of self-leveling mortar. *Journal of Cleaner Production*, 127 (2016) 204-213.
12. Hammas, Ines, Karima Horchani-Naifer, and Mokhtar Férid. Characterization and optical study of phosphogypsum industrial waste. *Stud. Chem. Process Technol.(SCPT)*, 1 (2013) 30-36.
13. X. Huang, Zhao, X., Bie, S., & Yang, C. Hardening performance of phosphogypsum-slag-based material. *Procedia Environmental Sciences*, 31 (2016) 970-976.
14. R. Moalla, Gargouri, M., Khmiri, F., Kamoun, L., & Zairi, M. Phosphogypsum purification for plaster production: A process optimization using full factorial design. *Environmental Engineering Research*, 23(1) (2017) 36-45.
15. F. A. López, Tayibi, H., García-Díaz, I., & Alguacil, F. J. Thermal dehydration kinetics of phosphogypsum. *Materiales de Construcción*, 65 (319) (2015)061.
16. S. Sebbahi, Chameikh, M. L. O., Sahban, F., Aride, J., Benarafa, L., & Belkbir, L. Thermal behaviour of Moroccan phosphogypsum. *Thermochimica Acta*, 302(1-2) (1997) 69-75.
17. A. A. Cuadri, Navarro, F. J., García-Morales, M., & Bolívar, J. P. Valorization of phosphogypsum waste as asphaltic bitumen modifier. *Journal of Hazardous materials*, 279 (2014) 11-16.
18. L. Ajam, Oueddou, M. B., Felfoul, H. S., & El Mensi, R. Characterization of the Tunisian phosphogypsum and its valorization in clay bricks. *Construction and Building Materials*, 23(10) (2009) 3240-3247.
19. S. Chouaya, M.A. Abbassi, Younes, R. B., & Zoulalian, A. Scrap Tires Pyrolysis: Product Yields, Properties and Chemical Compositions of Pyrolytic Oil. *Russian Journal of Applied Chemistry*, 91(10) (2018) 1603-1611.

(2019) ; <http://www.jmaterenvironsci.com/>